Original citation:
Haindl, Silvia, Kidszun, Martin and Kampert, Erik. (2017) Iron pnictide thin films : synthesis and physics. physica status solidi (b), 254 (1). 1600341.

Permanent WRAP URL:
http://wrap.warwick.ac.uk/87957

Copyright and reuse:
The Warwick Research Archive Portal (WRAP) makes this work by researchers of the University of Warwick available open access under the following conditions. Copyright © and all moral rights to the version of the paper presented here belong to the individual author(s) and/or other copyright owners. To the extent reasonable and practicable the material made available in WRAP has been checked for eligibility before being made available.

Copies of full items can be used for personal research or study, educational, or not-for profit purposes without prior permission or charge. Provided that the authors, title and full bibliographic details are credited, a hyperlink and/or URL is given for the original metadata page and the content is not changed in any way.

Publisher's statement:
"This is the peer reviewed version of the following article: Haindl, Silvia, Kidszun, Martin and Kampert, Erik. (2017) Iron pnictide thin films : synthesis and physics. physica status solidi (b), 254 (1). 1600341 which has been published in final form at http://dx.doi.org/10.1002/pssb.201600341 This article may be used for non-commercial purposes in accordance with Wiley Terms and Conditions for Self-Archiving."

A note on versions:
The version presented here may differ from the published version or, version of record, if you wish to cite this item you are advised to consult the publisher's version. Please see the 'permanent WRAP URL' above for details on accessing the published version and note that access may require a subscription.

For more information, please contact the WRAP Team at: wrap@warwick.ac.uk

warwick.ac.uk/lib-publications

Iron pnictide thin films: Synthesis and Physics

Silvia Haindl[*,1], **Martin Kidszun**[2], **Erik Kampert**[3]

[1] Physikalisches Institut, Universität Tübingen, Auf der Morgenstelle 14, 72076 Tübingen, Germany
[2] *previous address:* Leibniz Institute for Solid State and Materials Science, Helmholtzstr. 20, 01069 Dresden, Germany
[3] Dresden High Magnetic Field Laboratory (HLD-EMFL), Helmholtz-Zentrum Dresden-Rossendorf, 01328 Dresden, Germany

[*] Corresponding author: e-mail silvia.haindl@uni-tuebingen.de, Phone: +49-(0)7071-29 78619, Fax: +49-(0)7071-29 5373

Superconducting thin films play a prominent role in applications of superconductivity and provide an essential source for studying physical phenomena. Here we summarize the activities for iron pnictide thin films that were made during the German Special Priority Programme from 2009 until today. The quick availability of films after the discovery of superconductivity in the iron based superconductors enabled a number of experiments. After a general introduction and a brief historical overview we focus on film synthesis of iron pnictides by a two-step method and by pulsed laser deposition, the assessment of their application potential, the upper critical fields in iron oxypnictides of F-doped LaOFeAs and F-doped $Sm_{1-x}La_x$OFeAs and on superconductivity in $Fe/BaFe_2As_2$ heterostructures.

1 Introduction Superconducting thin film research is often categorized as materials research with emphasis on film growth, materials characterization and the development of applications. As a result, the topic of superconductivity in thin films finds itself sometimes reduced to questions in engineering and technology and less attention is paid to the capability to contribute fundamentally to problems in condensed matter physics. Latter focus offers two main philosophies: First, physics of thin films provide a test bed to study new mechanisms that occur due to reduced dimensionality or the appearance of interfaces. This can be, for example, observed in the recently developed FeSe monolayers being increasingly discussed.[1] Second, physics with thin films not only adds fundamental knowledge about material properties but also about the phenomena of superconductivity itself. Iron pnictide thin films thus provide fruitful insights into multiband superconductivity, the superconducting energy gaps or the order parameter symmetry.

Let us recall that thin films have constantly played an important role in the science of superconductors. Essential experiments were carried out on thin films, for example, the transmission of infrared light by Michael Tinkham[2] or electron tunnelling experiments by Ivar Giaever[3]. Both have confirmed the existence of the superconduct-ing energy gap, a fundamental quantity in the Bardeen-Cooper-Schrieffer (BCS) theory of superconductivity.[4] A further famous experiment based on superconducting thin films, the tricrystal experiment by Tsuei *et al.*, has proven in an impressive manner the *d-wave* symmetry of the superconducting order parameter in $YBa_2Cu_3O_{7-\delta}$.[5] Thin films of newly discovered superconducting materials – such as the iron pnictides – enable a number of studies from basic to advanced level. The immanent advantage of thin films compared to bulk material is the experimental access to critical currents due their reduced cross section. Dimensional reduction appears not only because of reduced thickness but can also be fabricated laterally by application of developed etching technologies. Thin films are, therefore, first choice for the access of the highest possible current densities in superconductors, the depairing critical current densities. Furthermore, films offer the possibility to investigate basic superconducting quantities and length scales such as penetration depth and coherence length, vortex physics, and non-equilibrium processes.

Here we want to focus on iron pnictide thin films, mainly iron oxypnictides grown in a *two-step synthesis*, Co-doped $BaFe_2As_2$ films and $Fe/BaFe_2As_2$ heterostructures that were grown by ultra-high-vacuum (UHV) pulsed laser deposition (PLD).[6] After a brief historical synopsis in

chapter 2, we address film growth of iron pnictides in chapter 3. In the main part of chapter 4 we give an overview of fundamental studies performed with iron pnictide thin films so far and exemplary discuss two examples of current interest: the upper critical field in iron oxypnictides and their anisotropies, and the modified electronic phase diagram and superconducting properties in Fe/BaFe$_2$As$_2$ heterostructures. The topic *Thin films of iron based superconductors* and the number of publications related to it grow continuously. It is, therefore, impossible to acknowledge all of the studies on iron pnictides. For topics of thin films of iron based superconductors (iron pnictides and iron chalcogenides) beyond the scope of this contribution the reader is referred to the following recent review articles: iron chalcogenide thin films and their superconducting properties,[7] molecular beam epitaxy (MBE) of K-doped BaFe$_2$As$_2$ and F-doped SmOFeAs films,[8] MBE of FeSe and K$_x$Fe$_{2-y}$Se$_2$,[9], and analytical characterization of thin films.[10]

2 Historical overview The announcement of a superconducting transition at 26 K in the F-doped iron oxypnictide compound LaOFeAs in 2008 has decisively influenced condensed matter physics.[11] LaOFeAs crystallizes in the ZrCuSiAs-type structure that is shortly called *1111*.[12] Excitement in Germany was even more fanned because many of the arsenic oxide and phosphide oxide compounds of the same structure-type were prepared and characterized at the university of Münster already during the 1990s.[13,14] Superconductivity in LaOFeP was found by PhD student Barbara Zimmer, but its discovery was not reported in a scientific journal. It was rediscovered independently by Kamihara in 2006 [15] and finally commented by Jeitschko in 2008.[16]
Shortly after the discovery of superconducting LaO$_{1-x}$F$_x$FeAs the F-doped iron oxypnictides were called *the hottest thing in superconductivity*.[17] Within the first half of 2008 many laboratories around the world started with the synthesis of iron oxypnictides. When Chinese researchers raised the transition temperature to 55 K in F-doped SmOFeAs [18] everybody was reminded of the story of the high-T_c cuprates and a further *explosion* in T_c was expected. Soon it was recognized that, in terms of structure, the Fe$_2$As$_2$ layers played the important role for superconductivity. Consequently, new compounds with Fe$_2$As$_2$ layers in their unit cells were quickly found and tested successfully for superconductivity: K-doped BaFe$_2$As$_2$ (T_c = 38 K) [19], LiFeAs (T_c = 18 K) [20] and FeSe (T_c = 8 K) [21] that are shortly called *122-*, *111-* and *11*-compounds, respectively. Additional ingredients for the excitement came from theoretical work on the electronic band structure that underlined the multiband character of superconductivity [22] and proposed an unconventional order parameter symmetry called s$\pm$ with sign-changing phase between different Fermi sheets.[23]

2.1 Begin of iron pnictide film growth in 2008 and 2009 A handful of institutes worldwide started with iron pnictide thin film growth during 2008 and 2009. In Germany, a Special Priority Programme on iron-based superconductors funded by the German Research Foundation (DFG), started in 2009, offered a chance to get quickly into business with synthesis and investigation of the basic superconducting properties. At that time thin film growth of F-doped iron oxypnictide LaOFeAs had already started, and it soon turned out to be very difficult because an *in-situ* pulsed laser deposition (PLD) process seemed not be applicable. *In-situ* PLD experiments in Tokyo Institute of Technology resulted in epitaxial thin films without an expected superconducting transition due to a complete loss of fluorine doping.[24] An alternative approach was followed at IFW Dresden. After unsuccessful *in-situ* PLD experiments, a *two-step synthesis* based on an *ex-situ* heat treatment resulted in the first superconducting LaO$_{1-x}$F$_x$FeAs thin films.[25] As a consequence, further optimization was carried out at IFW Dresden, whereas Hidenori Hiramatsu and Takayoshi Katase at Tokyo Institute of Technology switched to PLD growth of subsequently found Co-doped SrFe$_2$As$_2$ and BaFe$_2$As$_2$ compounds.[26,27]
Nevertheless, the fast progress in the research of iron pnictides and the monthly discovery of several new superconducting pnictide compounds made it attractive and necessary to start with the synthesis of thin films based on BaFe$_2$As$_2$ in Germany, too. Co-doped SrFe$_2$As$_2$ films were successfully grown by *in-situ* PLD [26,28] but the films contained a large number of impurity phases, especially Fe and Fe-As. Co-doped BaFe$_2$As$_2$ instead was expected to be grown with higher purity and also easily by *in-situ* PLD. Indeed, Co-doped BaFe$_2$As$_2$ thin films could be grown epitaxially on a large number of commonly used oxide substrates and films showed superconducting even in the case of arsenic deficiencies or structural disorder. The fact that BaFe$_2$As$_2$ (as well as FeSe$_{1-x}$Te$_x$ as confirmed for crystals in Ref.[29]) contains a certain *robustness of superconductivity* against structural disorder was definitely a reason for the increased activities in *122* (and later *11*) thin film growth. In other words, despite deviations in thin film lattice parameters from the bulk and definitely a certain degree of disorder in atomic coordinates - exact coordinates of As and P (or Se and Te) atoms in the unit cells are not easily accessible - films were superconducting. Another reason why Co-doped BaFe$_2$As$_2$ thin films could be grown quickly was that neither a new sophisticated method for an initial PLD growth nor a time-consuming two-step synthesis like for the iron oxypnictides was required. Reports from research laboratories at Tokyo Institute of Technology (Hosono's lab) and at University of Wisconsin (Eom's lab) announced successful growth of Co-doped BaFe$_2$As$_2$ films under UHV and under HV conditions.[27,30]
It should be mentioned that simultaneously PLD growth of iron chalcogenides, FeSe, FeSe$_{1-x}$Te$_x$ and FeTe$_{1-x}$S$_y$ started in some thin film laboratories in Japan, China and

the USA.[31–33] In the following years thin film growth by PLD focused basically on Co-and P-doped $BaFe_2As_2$ and on $FeSe_{0.5}Te_{0.5}$. Because of less technical difficulties expected in an *in-situ* PLD process and the immediate advantage of a large number of possible superconducting compounds in the series of transition metal substituted $BaFe_2As_2$, Co-doped $BaFe_2As_2$ seemed a natural choice for a continuation of efforts within the research at IFW Dresden in 2009.

2.2 Progress in iron pnictide thin film growth and application potential for thin films Further progress was made in iron pnictide film growth, in the *two-step synthesis* for iron oxypnictides as well as in UHV-PLD of Co-doped $BaFe_2As_2$. The superconducting transition temperature for iron oxypnictide thin films was improved to 25 K for F-doped LaOFeAs, and finally, also epitaxial film growth of iron oxypnictides was achieved. As a result, thin films were used in investigations of fundamental superconducting properties. For example, weak-link behavior of grain boundaries was determined first in HV PLD grown Co-doped $BaFe_2As_2$ [30] and in polycrystalline $LaO_{1-x}F_xFeAs$ thin films.[35]

The film/substrate interface of iron pnictide films often contains a chemical reaction layer. In iron oxypnictide thin films a LaOF impurity phase formed at the film/substrate interface. The crystalline properties of the LaOF layer finally determine further heteroepitaxial or polycrystalline growth of the iron pnictide layer. Similarly, reaction layers were confirmed also for Co-doped $BaFe_2As_2$ thin films grown on $(La,Sr)(Al,Ta)O_3$ substrates, where a 2-3 nm thin Fe layer and Ba diffusion into the substrate was found by high resolution transmission electron microscopy. Interfacial reaction layers alter the lattice mismatch between substrate and film and can lead to strain relaxation. In iron pnictides interfaces are rarely clean or perfectly coherent, therefore, claims of *epitaxial strain* are often unsubstantiated and unconfirmed. An investigation of residual stresses in iron pnictide thin films is missing up to date.

Experiments carried out for Co-doped $BaFe_2As_2$ films on bicrystalline substrates revealed a less severe decrease of critical current densities with increasing mismatch angle of the grain boundary compared to $YBa_2Cu_3O_{7-\delta}$ thin films.[34] Nevertheless, grain boundaries with mismatch angles larger than 9° constrain the current flow through the film and act as weak-links mainly because of the small coherence lengths in the order of 1-3 nm in iron pnictides. In 2011 it was demonstrated that Co-doped $BaFe_2As_2$ can be deposited on flexible metallic substrates which are well-known precursors for the second generation high-T_c wires (coated conductors).[36,37] The comparison of (depinning) critical current densities at liquid helium temperature in *122* thin films demonstrates an improvement of nearly two orders of magnitude from 10^4 to 10^6 Acm^{-2} between the years 2009 and 2014.[43] Today, because of the accumulated knowledge for Co-doped $BaFe_2As_2$ thin film growth compared to other iron based superconductors, the

relatively high critical current densities ($J_c > 1$ $MAcm^{-2}$ in self-field up to magnetic fields of several Tesla) compared to *powder-in-tube* (PIT) wires of the same or related compounds, a relatively small anisotropy of the upper critical field, $\gamma_{H_{c2}} \approx 2-5$, and a less drastic weak-link behavior compared to $YBa_2Cu_3O_{7-\delta}$ thin films, Co-doped $BaFe_2As_2$ thin films may be regarded as candidate material in future superconducting high-current applications. In a similar way, the application potential for PLD grown iron chalcogenide superconductors, $FeSe_{0.5}Te_{0.5}$, is discussed. At present the highest critical current densities are measured in UHV PLD grown P-doped $BaFe_2As_2$ thin films. At a temperature of 4 K they show J_c of 7 $MAcm^{-2}$ in self field and 1 $MAcm^{-2}$ in an external magnetic field of $\mu_0H = 9$ T. It is believed that dislocations serve as effective centers for flux line pinning in these films. In addition, the angular anisotropy of J_c was highly reduced by controlling film growth rates.[38] Noteworthy are also pinning studies in iron pnictide thin films that started to investigate the response to naturally grown or artificially introduced secondary phases in $BaFe_2As_2$. The secondary phases (indicated as $BaFeO_2$ in Ref.[39]) revealed a promising enhancement of the pinning force in higher magnetic fields with maxima around $\mu_0H \approx 11\pm2$ T.[40] Since 2010 there is specific interest in the improvement of vortex pinning in Co-doped $BaFe_2As_2$ thin films by secondary phases and in multilayer geometries.[41,42]

A closer inspection of the available feasibility studies between the years 2010 and 2014 however revealed open problems and certain drawbacks of the new superconductors that delay commercialization. They are easily ignored due to the tendency towards an overoptimistic rhetoric. Until today there are no successfully developed demonstrators for superconducting devices that would assist a powerful assessment of the application potential of Fe-based superconductors.

Of course we cannot forecast future developments but the actual weakness of most of the assessments of a reliable application potential is their restriction to only one parameter (for example, J_c) or a restricted set of selected parameters. For sure not all hurdles are even already identified. This was pointed out in a review where the gap between the claimed application potential and the realization of functional devices is critically remarked.[43] Among iron pnictides, Co- and P-doped $BaFe_2As_2$ films are mostly replicated, but strictly speaking, there is still a lack of exact reproducibility in PLD thin film growth of iron based superconductors. The problem arises mainly because of the presence of elements with high vapor pressure (volatile elements) like As and P. Furthermore, not only superconducting properties are relevant but also mechanical ones, especially for an industrial manufacturing of iron based superconductors into conductors for power transmission or into coils for magnetic field generation, for example. Nevertheless, iron-based superconductors are dealt as promising candidates for superconducting appli-

cations basically because of their large critical surface in the (T_c, H_{c2}, J_c) coordinate space.

At this point we should not forget that the development of brittle A15 superconductors took over decades from their discovery in the 1950s to first useful wire solutions in the 1970s and 1980s with still continuous efforts in their optimization.[44–48] The situation of Fe-based superconductors is however more difficult because there is a competition with conventional superconductors that are already in use in various applications (Nb, NbN, A15-superconductors), MgB_2 and cuprates (especially $YBa_2Cu_3O_{7-\delta}$ coated conductors). Therefore, a realistic time frame for technical device fabrication is at least beyond a decade.

It should be mentioned briefly that FeSe monolayers excite the community today because of their record critical temperatures up to 60 K.[49] The $FeSe/SrTiO_3$ system (with a special preparation of $SrTiO_3$) is studied *in-situ* predominantly by scanning tunneling microscopy and angle-resolved photoelectron spectroscopy. Superconductivity at even 100 K was announced in Ref.[50]. The monolayer physics has opened new directions in the research of Fe-based superconductors and it has revitalized the electron-phonon coupling as a possible scenario for high T_c, controversially discussed at present and with Mazin's words, posing a *riddle* to scientists.[1]

3 Thin film growth of iron pnictides

3.1 Two-step synthesis of iron oxypnictides Superconducting iron oxypnictide thin films were first grown by a *two-step synthesis*.[25] The synthesis involves a thin film deposition at room temperature and, as a second step, an *ex-situ* heat treatment of the precursor film together with a pressed pellet of the same composition in an evacuated silica glass tube. The presence of the additional pellet is crucial for the film stoichiometry. The method was reviewed in Ref.[51], therefore, we will only shortly comment on it here.

Following remarks are important: The room temperature deposition was carried out by PLD, which is used for the creation of nucleation centers on a substrate (precursor). However, PLD itself is not determining film growth and can be replaced by other deposition methods as demonstrated recently.[52] Furthermore, phase formation, epitaxy (the orientation of the crystallographic lattice of film grains with respect to the substrate lattice) and superconducting properties sensitively depend on the parameters of the heat treatment. As a consequence, iron oxypnictide thin films fabricated by the so-called *two-step process* have a microstructure similar to single crystals but strongly differ from columnar grain growth that is typically observed in films grown by PLD.

The *ex-situ* heat treatment is carried out with a simple heat profile starting with a slow heating ramp ($5°Cmin^{-1}$) to a temperature in the range of $940°C – 970°C$, holding the temperature for 5–7 hours, and cooling slowly
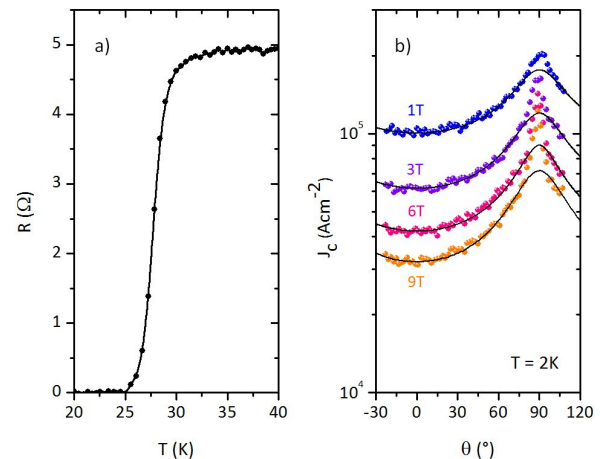

Figure 1 a) Resistive transition from normal to superconducting state in a $Sm_{1-x}La_xO_{1-y}F_yFeAs$ thin film. b) Angular dependence of critical currents in different magnetic fields at a temperature of 2 K. θ is defined as angle between the c-axis of the film and the direction of the applied magnetic field. The curves are fitted with an anisotropy $\gamma = 3.1$. J_c for magnetic fields applied parallel to film surface is increased due to enhanced vortex pinning. (See section 4.1.)

again to room temperature with ($-5°Cmin^{-1}$). Despite the long process of parameter optimization of the *ex-situ* heat treatment, finally the successful growth of polycrystalline and epitaxial $LaO_{1-x}F_xFeAs$ and $Sm_{1-x}La_xO_{1-y}F_yFeAs$ thin films provided a vital basis for investigations of the weak-link behavior of grain boundaries,[35] the determination of critical current densities [53] and a measurement of the superconducting gaps by means of point contact spectroscopy [54] and infrared optical measurements.[55] Given the difficulties in control and reproducibility of iron oxypnictide thin films, these first results can be regarded as invaluable for any further thin film investigations of iron-based superconductors.

Critical currents of the iron oxypnictide thin films grown in a two-step synthesis reached values of $10^5 Acm^{-2}$ in self-field at temperatures of 2 K. In Fig.1 we show exemplary the resistive transition of a $Sm_{1-x}La_xO_{1-y}F_yFeAs$ thin film with a T_{c90} of 29.5 K ($\Delta T_c = T_{c90} - T_{c10} = 2.9$ K, RRR = 2.1) and the angular dependence of the critical current densities in applied magnetic fields, $\mu_0H = 1$, 3, 6, and 9 T at 2 K.

The two-step synthesis of iron oxypnictide thin films with an ex-situ heat treatment is a time-consuming fabrication method compared to in-situ procedures, but growth of superconducting epitaxial films is possible. Until today only a few synthesis methods are available for the growth of iron oxypnictide thin films. The most recent success was made in *in-situ* PLD growth of iron oxypnictides.[56,57] To conclude, at present iron oxypnictides can be grown successfully by PLD, by a *two-step synthesis* method and also by MBE.[58].
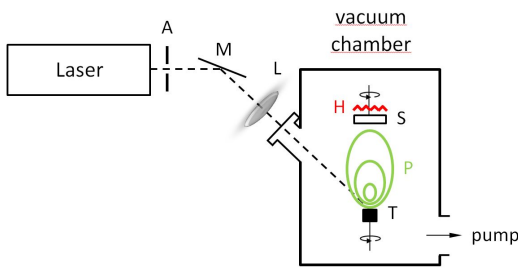
Figure 2 Pulsed laser deposition setup with laser beam optics (aperture - A, mirror - M, lense -L) a vacuum chamber with the source of material (target -T) a supporting medium for the as grown film (substrate - S), and a substrate heater - H for regulating the film growth temperature. During the PLD process a pulsed laser beam (dashed line) is used for heating, evaporation and ionization of the target material. The generated plasma plume - P propagates into the vacuum chamber towards the substrate.

3.2 UHV-PLD growth of BaFe$_2$As$_2$ and Fe/BaFe$_2$As$_2$ thin films with Co-doping PLD is a widely used thin film growth method because it is easy to handle.[59] A schematic drawing of a typical setup is given in Fig.2. PLD belongs to the group of vapor deposition methods with constituents of the vapor away from thermal equilibrium: inside a vacuum chamber material is transferred from a source (target) by means of plasma plume generated by a pulsed laser beam and deposited on substrates. PLD works amazingly well for a large number of materials, however, PLD becomes challenged when elements with low melting points and high vapor pressure are present in the material source. This is problematic for iron pnictide film growth, mainly for F-doped iron oxypnictides, but also for the 122 compounds where As deficiency is a subtle issue.

Co-doped BaFe$_2$As$_2$ films can be grown by UHV-PLD on different substrates and upon a relatively broad window of deposition parameters. It was furthermore shown in a recent study that the film quality of BaFe$_2$As$_2$ does not depend on the laser wavelength that is used for target ablation, however the energy of the laser pulse has decisive influence on the optimal growth rate.[60] Film growth at IFW Dresden was performed using a KrF excimer laser (λ = 248 nm) with energy densities on the target between 3 - 5 Jcm^{-2}.

Ideal deposition temperatures were found for Co-doped BaFe$_2$As$_2$ to be in the range 650°C to 700°C (at IFW Dresden). A slightly shifted temperature interval was found for the same compound at Tokyo Institute of Technology. For lower deposition temperatures the grown films do not obey a unique epitaxial relationship (cube-on-cube in most cases) and also contain misoriented grains with a 45° *in-plane* rotation between film and substrate unit cells.[61, 62] It should be mentioned that similar trends in epitaxial growth were observed in UHV-PLD of iron chalcogenide thin films.[63,64] Higher fabrication temperatures can result in off-stoichiometries, an enhanced amount of Fe

impurities, Fe-As impurities, As-deficiencies, and also defects (film cracking).

A more elaborate characterization of the film/substrate interface by high resolution transmission electron microscopy revealed, as mentioned above, a naturally occurring Fe layer with a structurally excellent matching between Fe and the BaFe$_2$As$_2$ crystallographic lattice. Interfacial Fe and cluster-like Fe impurities within the BaFe$_2$As$_2$ matrix are the result of As loss during film deposition and already indicate that stoichiometric transfer (from the target material to the substrate) is not fully guaranteed.

Nevertheless, the observation of an interfacial Fe layer triggered experiments of film growth on an intentionally grown Fe buffer layer and, thus, the fabrication of superconducting/ferromagnetic heterostructures.[65, 66] Because of the coherent Fe/BaFe$_2$As$_2$ interface and the proposed bonding between Fe and the Fe$_2$As$_2$ layer Thersleff conjectured that Fe would be a generic buffer layer for all Fe-based superconductors. Meanwhile this assumption cannot be confirmed for Fe-oxypnictides.[56,57]

At present and, in comparison with available results worldwide, growth of an Fe buffer layer is neither a necessary requirement nor free of disadvantages for the fabrication of BaFe$_2$As$_2$ films.[43] First, epitaxial growth of BaFe$_2$As$_2$ is achieved only with a certain thickness of the Fe buffer. If the Fe buffer layer is too thin, non-uniform, or characterized by island growth, c-axis orientation is reduced and inclined lattice orientations occur.[67] In order to prepare a relatively smooth Fe surface, Fe is deposited at room temperature and heated up to the deposition temperature of the Fe-pnictide compound. If the temperature, however, becomes too high, then cracking and dewetting of the thin films occur. This might be the case for a number of Fe/BaFe$_2$As$_2$ thin films grown on MgAl$_2$O$_4$ substrates (Fig. 3).

Besides the influence on grain growth, the Fe layer strongly influences film stoichiometry, and, more seriously, the distribution of Co doping level in BaFe$_2$As$_2$. Atomic probe tomography (APT) as well as Auger electron spectroscopy (AES) investigations have revealed that Co diffuses into the Fe-buffer during thin film growth leading to a non-uniform Co concentration across the film cross-section. In addition oxygen incorporation was found in Fe/BaFe$_2$As$_2$ multilayers.[43] The more subtle the characterization of thin films the more evident becomes the fact that BaFe$_2$As$_2$ film growth is not entirely trivial and off-stoichiometries or composition gradients exist. Conclusively, the high deposition temperatures above 700°C for Co-doped BaFe$_2$As$_2$ have detrimental influence on the film stoichiometry. Furthermore, interactions between the critical currents in the superconducting BaFe$_2$As$_2$ layer and the magnetization of the Fe layer could be demonstrated first by magneto-optical imaging of the trapped magnetic flux profile.[43]

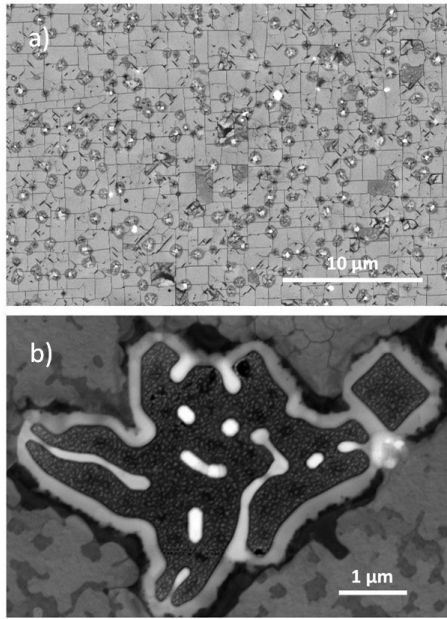In order to illustrate the differences in UHV-PLD growth

Figure 3 Scanning electron micrographs of a) film cracking and b) dewetting phenomena observed in Fe/BaFe$_2$As$_2$ and Fe/BaFe$_2$As$_2$/Fe/BaFe$_2$As$_2$ multilayers grown on MgAl$_2$O$_4$ at too high deposition temperature.

of Co-doped BaFe$_2$As$_2$ and iron oxypnictide films one has to realize the following: UHV-PLD growth of BaFe$_2$As$_2$ is comparable to the growth of intermetallic phases with typical parameters of high substrate temperatures and fast laser repetition rates. Control of stoichiometry, however, should limit the maximum growth temperature to around $700°C - 750°C$. In addition, Co-doping in the films can be controlled easier in PLD than doping with fluorine. A list of UHV PLD grown iron pnictide compounds are shown in Table 1.

Table 1 Iron pnictides grown by UHV PLD

compound	comment	Ref.
122		
CaFe$_{2-x}$Co$_x$As$_2$	impurity phases	[61]
SrFe$_{2-x}$Co$_x$As$_2$	impurity phases	[26]
Sr$_{1-x}$La$_x$Fe$_2$As$_2$	impurity phases	[68]
BaFe$_{2-x}$Co$_x$As$_2$	most investigated	[27]
BaFe$_{2-x}$Cr$_x$As$_2$	not superconducting	[62]
BaFe$_2$As$_{2-x}$P$_x$	highest J_c	[69]
Ba$_{1-x}$La$_x$Fe$_2$As$_2$	metastable compound	[70]
Ba$_{1-x}$RE$_x$Fe$_2$As$_2$	RE = Ce, Pr, Nd, Sm	[71]
1111		
SmO$_{1-x}$F$_x$FeAs		[56]

4 Fundamental studies on iron pnictide thin films

Studies using iron pnictide thin films have provided important information on the superconducting state. Thin films are convenient for a number of experiments on the superfluid density or the energy gap. Penetration depth measurements for Co-doped BaFe$_2$As$_2$ thin films by a two-coil mutual inductance apparatus have confirmed values in the range of $\lambda(0) = 350 - 430$ nm and, therefore, are fully comparable to values obtained for crystals.[72] The temperature-dependence of the superfluid density revealed by terahertz spectroscopy in BaFe$_2$As$_2$ was modeled by a two-band,[73] and later, by a three-band model.[74] Both of the mentioned experiments have found evidence for a small superconducting gap with $2\Delta(0)/k_BT_c \approx 2.1 - 2.2$. For low temperatures, $T \rightarrow 0$ the penetration depth $\Delta\lambda(T)/\lambda(0)$ can be described by a power-law $\propto (T/T_c)^n$ with exponent $n \approx 2$ [75] or $n \approx 2.5$.[72] Infrared spectroscopy on F-doped LaOFeAs thin films grown by a *two-step synthesis* revealed a nodeless superconducting gap.[55]

PLD thin film growth offers also advantages in the stabilization of new metastable phases. La-doped BaFe$_2$As$_2$ is believed to be structurally unstable due to a theoretically predicted high density of states at the Fermi level.[76] The compound could not yet be synthesized by conventional solid-state methods, however by PLD film growth.[70] This film study is of interest, because it confirms that BaFe$_2$As$_2$ iron pnictides can be charge-carrier doped either directly, by substitution in the Fe$_2$As$_2$-layers (Co-substitution), or indirectly, by chemical substitution on the Ba-site (La-substitution). The resulting electronic phase diagram is nearly equivalent for both substitutions. Consequently, BaFe$_2$As$_2$ thin films doped with rare-earth (RE) elements containing 4f electrons were also successfully grown by PLD and thus offered the possibility to study interaction effects between the itinerant electron system of 3d electrons in BaFe$_2$As$_2$ and the localized 4f states of the RE substitutes. It was shown that superconducting transition temperatures decrease within the RE series: 22.4 K (La-doping), 13.4 K (Ce-doping), 6.2 K (Pr-doping) and 5.8 K (Nd-doping).[71]

4.1 Upper critical fields in iron oxypnictides

The high upper critical fields, H_{c2}, of F-doped iron oxypnictides immediately provoke a number of questions related to the responsible limitation mechanism for superconductivity. A non-negligible anisotropy in iron pnictides is expected because of the layered structure with successively stacked FeAs and LaO ([RE]O) layers. Consequently, the upper critical fields should differ for magnetic fields applied along the *c*-axis of the unit cell, $H_{c2,c}$ from upper critical fields with magnetic field in the basal plane, $H_{c2,ab}$.[77] Surprisingly, the anisotropy becomes quite small in *122* iron pnictides and tends even to $\gamma_{Hc2} = H_{c2,ab}/H_{c2,c} = 1$ (called *pseudo-isotropic*) for small temperatures near $T \rightarrow 0$ as it was shown in an early

study on Co-doped $SrFe_2As_2$ thin films.[78]

In the iron oxypnictides, H_{c2} is less drastically pseudoisotropic, although γ_{Hc2} decreases with decreasing temperature. Experimentally, the high H_{c2} values are challenging, especially at low temperatures. In such a case, measurements performed with conventional laboratory equipment in magnetic fields up to $5 - 9$ T only access a very limited range of the magnetic phase diagram of these extreme type-II superconductors and they are not able to confirm or rule out theoretical predictions on the temperature-dependence of H_{c2}. Pulsed magnetic fields are required in order to obtain magnetic fields beyond 50 and 60 T. There is, therefore, current interest in the measurement of H_{c2}, γ_{Hc2} and their temperature dependence in magnetic fields up to 70 T. Table 2 summarizes extrapolated values of the upper critical fields at $T = 0$ K for selected F-doped iron oxypnictides.

As mentioned in a previous review [43] epitaxially grown iron oxypnictide thin films offered the unique possibility for the investigation of the anisotropic superconducting properties. Until today the single crystal growth of these materials is extremely difficult and rare, because it requires high pressure synthesis.[82]

Upper critical fields of $LaO_{1-x}F_xFeAs$ and $Sm_{1-x}La_xO_{1-y}F_yFeAs$ thin films are shown for both magnetic field orientations, $H \parallel c$ and $H \parallel ab$ in Fig.4. Interestingly, there is no clear tendency for saturation at low temperatures and upward curvatures are found. Theoretical work has ever since shown that the temperature dependence of H_{c2} provides important information. In general, it is governed by the anisotropy of the electronic structure (Fermi surface) and the anisotropy of the energy gap of the superconductor. Furthermore, H_{c2} provides knowledge about the robustness of the superconducting state in magnetic fields and on the mechanisms responsible for Cooper-pair breaking.

The temperature dependence of $H_{c2}(T)$ of F-doped iron oxypnictides deviates from the Werthamer-Helfand-Hohenberg (WHH) [83] description. This description was derived for isotropic conventional (and single band) superconductors. Practically all conditions are not valid for iron pnictides and deviations are a signature of anisotropy and multiband superconductivity, similarly to the observations made for MgB_2 in the dirty limit.[84] Previously, we have found fits according to a model developed by Gurevich for two-band superconductivity [85] where we assumed two decoupled electronic bands and a strong difference between the diffusivities in the two bands ($D_2/D_1 < 1$) in order to model the strong upward curvature at low temperatures in Ref.[51]

In addition the upper critical field anisotropy was extracted from angular dependent critical current density measurements upon application of a special formalism developed by Blatter, Geshkenbein and Larkin called *anisotropic Ginzburg-Landau scaling*.[86] This approach is based on a mapping between anisotropic superconductors ($H_{c2}(\phi)$
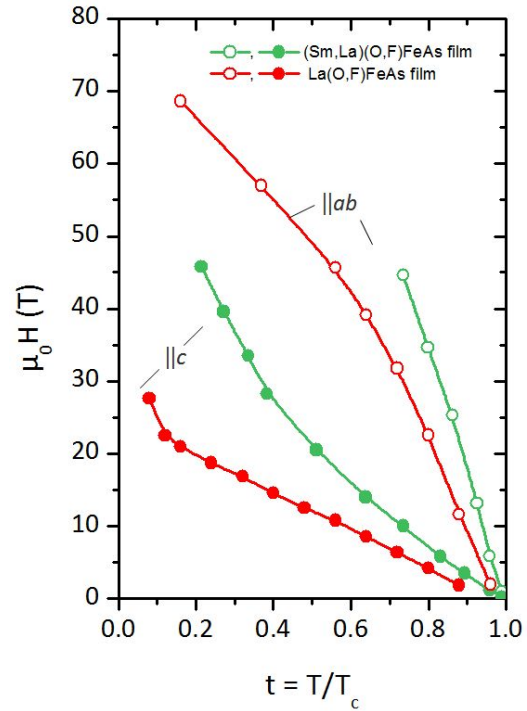

Figure 4 Upper critical fields, $\mu_0 H_{c2,c}$ (closed symbols) and $\mu_0 H_{c2,ab}$ (open symbols) versus reduced temperature compared for a $LaO_{1-x}F_xFeAs$ thin film of $T_c = 25.0$ K (red curves) and a $Sm_{1-x}La_xO_{1-y}F_yFeAs$ thin film of $T_c = 31.3$ K (green curves) fabricated by a *two-step synthesis*.

ellipse in polar coordinates) and isotropic superconductors ($H_{c2}(\phi)$ circle in polar coordinates). The formalism defines an effective magnetic field,

$$H_{eff} = H\sqrt{cos^2(\phi) + \frac{1}{\gamma^2}sin^2(\phi)} \qquad (1)$$

where $\gamma = m_c/m_{ab}$ is the effective mass anisotropy and ϕ is the angle between the direction of the applied magnetic field and the c-axis of the superconductor. Here, γ is the only fit parameter that should regulate the overlap of the measured angular dependent critical current densities $J_c(H, \phi) \equiv J_c(H_{eff})$. For simplicity we have assumed that the effective masses include only band structure anisotropies and not energy gap anisotropies. We found an excellent applicability of this mapping scheme over a large angle range due to the fact that flux pinning in the here investigated superconducting films ($J_c < 10^5 Acm^{-2}$) is basically controlled by the vortex core size and point-like defects. Details can be found in Ref.[51].

We want to mention here again, that the extracted anisotropy from the upper critical fields, γ_{Hc2} and the anisotropy γ found as parameter in the *anisotropic Ginzburg-Landau scaling* approach are a priori not equivalent because, in general, there are two contributions to the angular dependence (anisotropy) of depinning critical

Table 2 Extrapolated values of the upper critical field of oxypnictides at $T = 0$ K for a magnetic field applied parallel to the c-axis ($H_{c2,c}(0)$) and perpendicular to the c-axis ($H_{c2,ab}(0)$). $\star$ this work

compound	$T_{c,90}$	$\mu_0 H_{c2,c}(0)$	$\mu_0 H_{c2,ab}(0)$	sample	Ref.
$LaO_{0.9}F_{0.1}FeAs$	28 K	41 T	62 T	polycrystalline	[79]
$LaO_{1-x}F_xFeAs$	25 K	40 T	77 T	thin film	$\star$
$NdO_{0.7}F_{0.3}FeAs$	46 K	>60 T	>120 T	single crystal	[80]
$SmO_{0.9}F_{0.1}FeAs$	42 K	50 T	100 T	single crystal	[81]
$Sm_{1-x}La_xO_{1-y}F_yFeAs$	31 K	>50 T	>90 T	thin film	$\star$
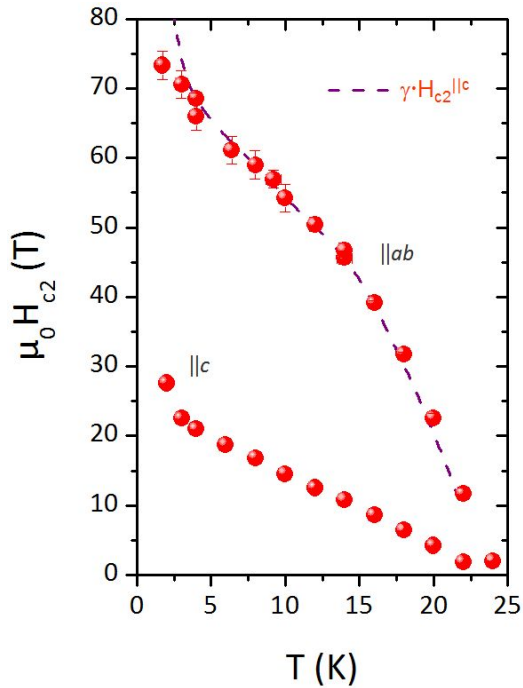
Figure 5 Temperature dependence of the upper critical field, $\mu_0 H_{c2,c}$ and $\mu_0 H_{c2,ab}$ for a $LaO_{1-x}F_xFeAs$ thin film measured down to 1.8 K (same as in Fig. 4 with more data points for clarity). Values above magnetic fields of 70 T are extrapolations from $R(\mu_0 H)$ measurements. The dashed line (*prediction*) is the product of $\mu_0 H_{c2,c}$ as given in this graph with the fit parameter γ obtained from the mapping in the *anisotropic Ginzburg-Landau scaling approach* (as described in the text). We find an excellent correspondence between the measured values for $\mu_0 H_{c2,ab}$ up to 70, T and the *prediction* made by critical current measurements.

current densities. First, the anisotropy in J_c depends on the vortex core size variation that is governed by angular variation of coherence lengths (ξ_c/ξ_{ab}). Second, $J_c(\phi)$ also can depend on the variation of the flux pinning energy, and, therefore, on the angular variation of the vortex line energies that are proportional to (λ_{ab}/λ_c). Latter contribution increases with larger defects but is negligible for small and point-like defects. Whenever the second contribution becomes non-negligible, the mapping scheme from the anisotropic Ginzburg-Landau scaling fails and results

in an incomplete overlap of critical current density curves versus the effective magnetic field (see Ref. [87]). More importantly, it is unclear how the fit parameter γ is then connected with the H_{c2}- (or electronic mass) anisotropy. Therefore, the *anisotropic Ginzburg-Landau scaling* is not the best tool for an investigation of flux line pinning. Its application will not provide a conclusive answer except about the presence or absence of directionally acting pinning centers.

The films synthesized by the *two-step method* contain only point-like and randomly distributed defects and clearly lack strong oriented or spatially extended pinning centers that would force flux lines to be pinned along specific directions apart from the usually increased pinning along the film (or substrate) surface ($H \parallel ab$). Transmission electron microscopy has confirmed a microstructure without secondary phase inclusions within the superconducting 1111 matrix. Accordingly, we found a perfect overlap of critical current densities versus the effective magnetic field.[53] A detailed discussion is already given in Ref.[51], but it should be pointed out here again, that in this special case, the anisotropy of the upper critical field can be extracted especially at low temperatures, where critical currents are large. The value for γ can be used for a *prediction* of $H_{c2,ab}$ after a measurement of the smaller $H_{c2,c}$ (compare Fig.5), even if it is extracted from measurements in low magnetic fields (up to 9 T) only.

As a result, the temperature-dependent anisotropy of the upper critical field is in agreement with results for other iron pnictide superconductors.[88] The temperature dependence of $H_{c2,ab} = \gamma H_{c2,c}$, that was estimated, quickly exceeded the limit of conventional measurement devices (9 - 17 T cryostats). The obligatory experimental proof of the upper critical field anisotropy of $LaO_{1-x}F_xFeAs$ was finally obtained with electrical transport measurements in pulsed magnetic fields up to 70 T, with a pulse duration of about 150 ms, at Dresden High Magnetic Field Laboratory (HLD). In Fig.5 we show also the detailed temperature dependence of the upper critical field $H_{c2,ab}$. The fit parameter γ obtained by *anisotropic Ginzburg-Landau scaling* obviously corresponds to $\gamma_{Hc2} = H_{c2,ab}/H_{c2,c}$ (compare also Fig.6).

We have compared the upper critical field anisotropy of a $LaO_{1-x}F_xFeAs$ and a $Sm_{1-x}La_xO_{1-y}F_yFeAs$ thin film with available data for polycrystalline bulk and single crystals (Fig. 6). Our investigation shows that the anisotropy
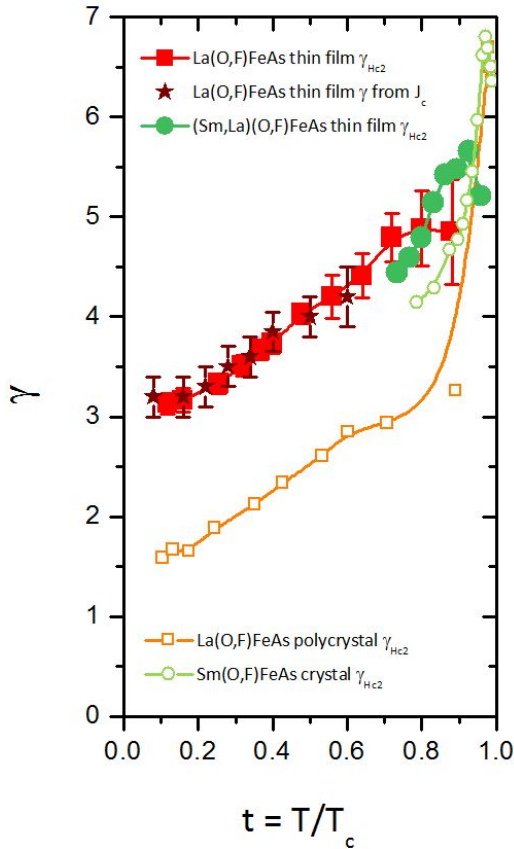
Figure 6 Temperature dependence of upper critical field anisotropies, γ_{Hc2}, in Fe-oxypnictide thin films (closed symbols) compared with data from bulk/crystal samples (open symbols) from Refs.[79,80]. Stars indicate γ obtained as the fit parameter in the anisotropic Ginzburg-Landau scaling applied to angular dependent critical current densities.

is underestimated when extracted from $T_{c,10}$ and $T_{c,90}$ criteria in the resistive transition of polycrystals.[79] The upper critical field anisotropy obtained from thin films ranges between 3 ($T \to 0$) and 5-6 ($T \to T_c$) reveals the mass anisotropies. Since the iron oxypnictide thin films grown by the *two-step method* are comparable to the quality of single crystals our investigation on the upper critical fields offers also reasonable quantitative comparisons. In all cases the anisotropy, γ_{Hc2}, increases with increasing temperature (with an approximate rate of $\approx 0.13/K$ in the interval between 5 K and 20 K). In the limits for $T \to 0$ and $T \to T_c$, the mass anisotropies of the dominant Fermi pockets can be extracted.[51]

As a final remark, we should mention that the discussions for H_{c2} and its anisotropy are basically carried out in the frames of two-band models, although the Fermi surface of iron pnictides shows that up to five bands can be involved. Furthermore, it is speculated if a Fulde-Ferrel-Larkin-Ovchinnikov (FFLO) phase can be stabilized due to

Pauli limitation or due the unconventional order parameter symmetry in the iron pnictides.

4.2 Critical temperature and upper critical fields in Fe/BaFe$_2$As$_2$ heterostructures The fabrication of a doping series ($x = 0 - 0.2$) of Ba(Fe$_{1-x}$Co$_x$)$_2$As$_2$ on Fe-buffered MgO(100) substrates indicated the interplay between stoichiometry, magnetism and strain.[89] The introduction of an Fe buffer revealed deviations from the electronic phase diagram compared to bulk samples or thin films grown without Fe buffer that asked for an explanation (Fig. 7).

Dopant inhomogeneities and As deficiency (As vacancies) were discussed as possible primary sources for the deviations in $T_c(x)$, and we have provided possible scenarios for the underdoped and the overdoped films. In nominally overdoped films, AES investigations have confirmed a concentration gradient of Co within in the Fe/Ba(Fe$_{1-x}$Co$_x$)$_2$As$_2$ bilayers. Co diffuses into the Fe buffer layer, an effect that occurs stronger with higher deposition temperatures and increased Co content. As a result, the superconducting layer is inhomogeneous in Co-doping and, therefore, inhomogeneous in its superconducting properties. Naturally, a layer with maximum T_c occurs that drives the overall T_c to higher temperatures. Therefore, deviations from the known electronic phase diagram on the overdoped branch with the higher T_c values can be explained easily by the inhomogeneous Co concentration.

The anomalous high critical temperature for underdoped Fe/Ba(Fe$_{1-x}$Co$_x$)$_2$As$_2$ thin films are of different origin. In addition, they cannot entirely be explained by the c-axis lattice variation or by an unquantified strain argument. A possible explanation was given by the first author, that the increase in critical temperature in the underdoped regime is possibly explained by a perturbation of the spin density wave (SDW) state, for example, due to impurity scattering. As-deficiency may play a role in this scenario, but in general, thin films grown by PLD can be regarded as more disordered. In perturbing the spin-density wave state in the underdoped regime an increased density of states at the Fermi level is provided which gives rise to higher superconducting critical temperatures.[93]

The slopes of the upper critical fields $\mu_0 H_{c2,ab}$ for Fe/Ba(Fe$_{1-x}$Co$_x$)$_2$As$_2$ bilayers increase linearly with increasing Co-doping, whereas the slopes of the upper critical fields $\mu_0 H_{c2,c}$ decrease slightly with increasing Co-doping (Fig. 8a). For single band superconductors the slopes $-dH_{c2,c}/dT$ are proportional to $T_c/ < v_{F,a}^2 >$ and $-dH_{c2,ab}/dT \propto T_c/(< v_{F,a}^2 >< v_{F,c}^2 >)^{1/2}$. Then, division of $-dH_{c2,ab}/dT$ by $-dH_{c2,c}/dT$ (the anisotropy of the H_{c2}-slopes), $\gamma^\star$, provides direct access to the electronic anisotropy (under the assumption of an isotropic superconducting gap again) and reduces to γ

$$(\gamma^\star)^2 \propto < v_{F,a}^2 > / < v_{F,c}^2 > = \gamma^2. \qquad (2)$$
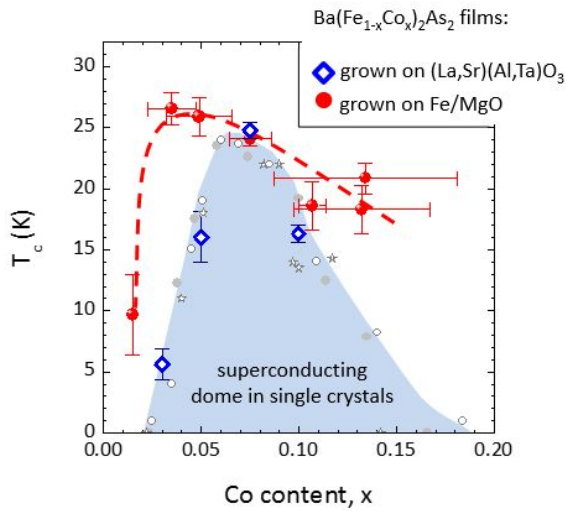
Figure 7 Modified electronic phase diagram for Fe/Ba(Fe$_{1-x}$Co$_x$)$_2$As$_2$ bilayers (Ref. [89]). The superconducting dome for the bilayers (indicated by red dashed line) is increased compared to the superconducting dome in single crystals, bulks (Refs. [90–92]) and thin films of Ba(Fe$_{1-x}$Co$_x$)$_2$As$_2$ grown on (La,Sr)(Al,Ta)O$_3$ substrates (Ref.[61]) (light blue area).

with $v_{F,a}$ and $v_{F,c}$ the corresponding Fermi velocities *in-plane* ($\parallel ab$) and *out-of-plane* ($\parallel c$).

In a two-band superconductor, however, the expressions for H_{c2} or dH_{c2}/dT are not so trivial anymore. Both, γ and $\gamma^\star$ are then functions of all $< v_{F,a}^2 >_i$ and $< v_{F,c}^2 >_i$ ($i = 1, 2$) and depend not only on the electronic anisotropy but also on the interband coupling strength. Consequently, the expression for γ is modified. Because these expressions are not available we will consider the limit of $T \to T_c$ here, where $\gamma = \gamma^\star$ and focus on the dependence on the doping content.

Fig.8b indicates an increase of $\gamma^\star$ with increasing Co-content. A similar trend can be estimated from γ measured in single crystals of Ba(Fe$_{1-x}$Co$_x$)$_2$As$_2$ with different Co-doping level.[94] The anisotropy for underdoped films is slightly higher compared to bulk samples, that may be attributed to a larger impurity scattering and, therefore, to slightly higher critical temperatures, T_c.[94] Another interesting fact was pointed out by Tanatar *et al.*[97] who argued an overall increase in the electronic anisotropy $\gamma^\star$ for non-relaxed z-positions of As ions in the unit cell. Therefore, not only Co-doping but also disorder in the As-sublattice has a non-negligible influence on the anisotropy as well.

A spin density state in underdoped samples impurity scattering can counterintuitively lead to an increase in T_c. Although this is only a vague comparison, it may serve as a qualitative explanation. A recent study on Ni substituted

BaFe$_2$As$_2$ single crystals emphasizes that the anisotropy is regulated by the interplay between impurity scattering and the evolution of Fermi surface topology.[98] However, in order to obtain a final conclusive picture and to rule out other mechanisms more detailed studies are necessary.

Conclusions To summarize, the growth of iron pnictide thin films today is mostly experienced with Co- and P-doped BaFe$_2$As$_2$. We have briefly reviewed the historical development. In the last years progress was made step-by-step in a better control of film growth and the improvement of superconducting properties, especially the critical current densities.

The availability of iron pnictide thin films allowed also a number of interesting and fundamental studies on the superconducting state. We have presented some of the thin film studies in general and selected topics that are currently of interest in iron pnictide research: the discussion of film growth and material aspects for possible superconducting applications, the upper critical field of oxypnictide thin films, and, finally, we have proposed a scenario how the electronic phase diagram is modified in heterostructures and commented the change in anisotropy with doping content.

References

[1] I. I. Mazin, Nature Mater. 14, 755 (2015)

[2] M. Tinkham, Phys. Rev. 104, 845 (1956)

[3] I. Giaever, Phys. Rev. Lett. 5, 147 (1960); Phys. Rev. Lett. 5, 464 (1960)

[4] J. Bardeen, L. N. Cooper, J. R. Schrieffer, Phys. Rev. 108, 1175 (1957)

[5] C. C. Tsuei et al., Phys. Rev. Lett. 73, 593 (1994)

[6] We will nevertheless mention iron chalcogenide thin films or other film growth methods whenever it provides a meaningful supplementary information in the context.

[7] P. Mele, Sci. Technol. Adv. Mater. 13, 054301 (2012)

[8] S. Ueda, S. Takeda, S. Takano, A. Mitsuda, M. Naito, Jpn. J. Appl. Phys. 51, 010103 (2012)

[9] L.-L. Wang, X.-C. Ma, X. Chen, Q.-K. Xue, Chin. Phys. B 22, 086801 (2013)

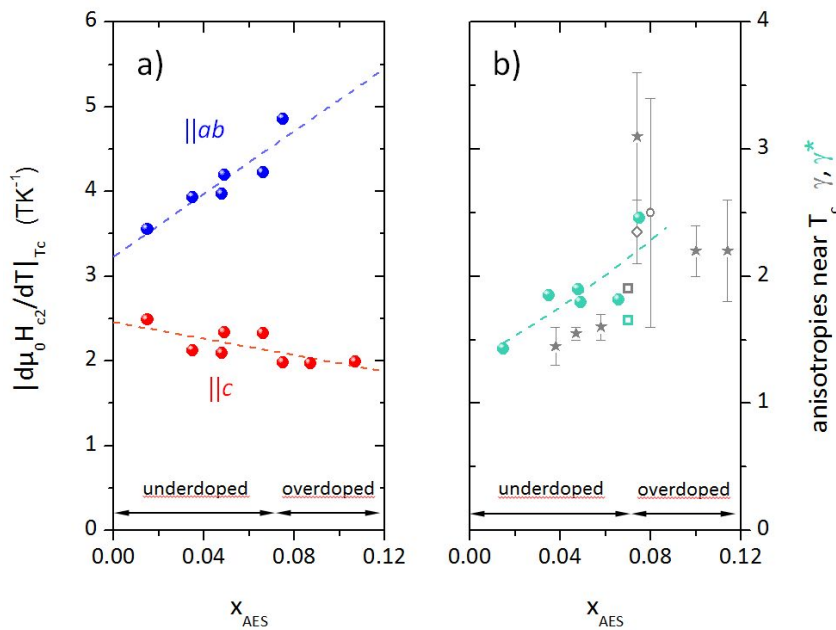[10] S. C. Speller, T. Mousavi, P. Dudin, Nov. Supercond. Mater. 1, 29 (2015)

Figure 8 (a) Slopes of the upper critical field near T_c for $\mu_0 H \parallel c$ (red closed symbols) and $\mu_0 H \parallel ab$ (blue closed symbols) measured in TK^{-1} and (b) their anisotropy, $\gamma^\star$, (open symbols, right scale) as defined in the text for Fe/Ba(Fe$_{1-x}$Co$_x$)$_2$As$_2$ bilayers with different $x = x_{AES}$ determined by AES. The obtained values are compared to γ (gray symbols) and $\gamma^\star$ (cyan symbols) values for Ba(Fe$_{1-x}$Co$_x$)$_2$As$_2$ available in literature (stars[94], circle[95], square[96], diamond[97]).

[11] Y. Kamihara, T. Watanabe, M. Hirano, H. Hosono, J. Am. Chem. Soc. 130, 3297 (2008)

[12] V. Johnson, W. Jeitschko, J. Solid State Chem. 11, 161 (1974)

[13] B. I. Zimmer, W. Jeitschko, J. H. Albering, R. Glaum, M. Reehuis, J. Alloys Comp 229, 238 (1995)

[14] P. Quebe, L. J. Terbüchte, W. Jeitschko, J. Alloys Comp. 302, 70 (2000)

[15] Y. Kamihara, H. Hiramatsu, M. Hirano, R. Kawamura, H. Yanagi, T. Kamiya, H. Hosono, J. Am. Chem. Soc. 128, 10012 (2006)

[16] W. Jeitschko, B. I. Zimmer, R. Glaum, L. Boonk, U. Ch. Rodewald, Z. Naturforsch. 63b, 934 (2008)

[17] Editors Summary in Nature 453 (15 May 2008) download at *http://www.nature.com/nature/journal/v453/n7193/edsumm/e080515-11.html*

[18] Z.-A. Ren, W. Lu, J. Yang, W. Yi, X.-L. Shen, Z.-C. Li, G.-C. Che, X.-L. Dong, L.-L. Sun, F. Zhou, Z.-X. Zhao, Chin. Phys. Lett. 2008, 25, 2215.

[19] M. Rotter, M. Tegel, D. Johrendt, Phys. Rev. Lett. 101, 107006 (2008)

[20] X. C. Wang, Q. Q. Liu, Y. X. Lv, W. B. Gao, L. X. Yang, R. C. Yu, F. Y. Li, C. Q. Jin, Solid State Commun. 148, 538 (2008)

[21] F.-C. Hsu, J.-Y. Luo, K.-W. Yeh, T.-K. Chen, T.-W. Huang, Ph. M. Wu, Y.-C. Lee, Y.-L. Huang,, Y.-Y. Chu, D.-C. Yan, M.-K. Wu, PNAS 105, 38 (2008)

[22] D. J. Singh, M.-H. Du, Phys. Rev. Lett. 100, 237003 (2008)

[23] I. I. Mazin, D. J. Singh, M. D. Johannes, M. H. Du, Phys. Rev. Lett. 101, 057003 (2008)

[24] H. Hiramatsu, T. Katase, T. Kamiya, M. Hirano, H. Hosono, Appl. Phys. Lett. 93, 162504 (2008)

[25] E. Backen, S. Haindl, T. Niemeier, R. Hühne, T. Freudenberg, J. Werner, G. Behr, L. Schultz, B. Holzapfel, Supercond. Sci. Technol. 21, 122001 (2008)

[26] H. Hiramatsu, T. Katase, T. Kamiya, M. Hirano, H. Hosono, Appl. Phys. Express 1, 101703 (2008)

[27] T. Katase, H. Hiramatsu, H. Yanagi, T. Kamiya, M. Hirano, H. Hosono, Solid State Commun. 149, 2121 (2009)

[28] E.-M. Choi, S.-G. Jung, N. H. Lee, Y.-S. Kwon, W. N. Kang, D. H. Kim, M.-H. Jung, S.-I. Lee, L. Sun, Appl. Phys. Lett. 95, 062507 (2009)

[29] M. Tegel, C. Löhnert, D. Johrendt, Solid State Commun. 150, 383 (2010)

[30] S. Lee, J. Jiang, J. D. Weiss, C. M. Folkman, C. W. Bark, C. Tarantini, A. Xu, D. Abraimov, A. Polyanskii, C. T. Nelson, Y. Zhang, S. H. Baek, H. W. Jang, Y. Yamamoto, F. Kametani, X. Q. Pan, E. E. Hellstrom, A. Gurevich, C. B. Eom, D. C. Larbalestier, Appl. Phys. Lett. 95, 212505 (2009)

[31] Y. Han, W. Y. Li, L. X. Cao, S. Zhang, B. Xu, B. R. Zhao, J. Phys. Condens. Matter 21, 235702 (2009)

[32] W. Si, Z.-W. Lin, Q. Jie, W.-G. Yin, J. Zhou, G. Gu, P. D. Johnson, Q. Li, Appl. Phys. Lett. 95, 052504 (2009)

[33] P. Mele, K. Matsumoto, Y. Haruyama, M. Mukaida, Y. Yoshida, T. Kiss, Appl. Phys. Express 2, 073002 (2009)

[34] T. Katase, Y. Ishimaru, A. Tsukamoto, H. Hiramatsu, T. Kamiya, K. Tanabe, H. Hosono, Nat. Commun. 2, 409 (2011)

[35] S. Haindl, M. Kidszun, A. Kauffmann, K. Nenkov, N. Kozlova, J. Freudenberger, T. Thersleff, J. Hänisch, J. Werner, E. Reich, L. Schultz, B. Holzapfel, Phys. Rev. Lett. 104, 077001 (2010)

[36] K. Iida, J. Hänisch, S. Trommler, V. Matias, S. Haindl, F. Kurth, I. Lucas del Pozo, R. Hühne, M. Kidszun, J. Engelmann, L. Schultz, B. Holzapfel, Appl. Phys. Express 4, 013103 (2011)

[37] T. Katase, H. Hiramatsu, V. Matias, C. Sheehan, Y. Ishimaru, T. Kamiya, K. Tanabe, H. Hosono, Appl. Phys. Lett. 98, 242510 (2011)

[38] H. Sato, H. Hiramatsu, T. Kamiya, H. Hosono, Appl. Phys. Lett. 104, 182603 (2014)

[39] Y. Zhang, C. T. Nelson, S. Lee, J. Jiang, C. W. Bark, J. D. Weiss, C. Tarantini, C. M. Folkman, S.-H. Baek, E. E. Hellstrom, D. C. Larbalestier, C.-B. Eom, X. Pan, Appl. Phys. Lett. 98, 042509 (2011)

[40] C. Tarantini, S. Lee, Y. Zhang, J. Jiang, C. W. Bark, J. D. Weiss, A. Polyanskii, C. T. Nelson, H. W. Jang, C. M. Folkman, S. H. Baek, X. Q. Pan, A. Gurevich, E. E. Hellstrom, C. B. Eom, D. C. Larbalestier, Appl. Phys. Lett. 96, 142510 (2010)

[41] S. Lee, C. Tarantini, P. Gao, J. Jiang, J. D. Weiss, F. Kametani, C. M. Folkman, Y. Zhang, X. Q. Pan, E. E. Hellstrom, D. C. Larbalestier, C. B. Eom, Nature Mater. 12, 392 (2013)

[42] M. Miura, B. Maiorov, T. Kato, T. Shimode, K. Wada, S. Adachi, K. Tanabe, Nature Commun. 4, 2499 (2013)

[43] S. Haindl, M. Kidszun, S. Oswald, C. Hess, B. Büchner, S. Kölling, L. Wilde, T. Thersleff, V. V. Yurchenko, M. Jourdan, H. Hiramatsu, H. Hosono, Rep. Prog. Phys. 77, 046502 (2014)

[44] G. F. Hardy, J. K. Hulm, Phys. Rev. 93, 1004 (1954)

[45] J. E. Kunzler, E. Buehler, F. S. L. Hso, J. H. Wernick, Phys. Rev. Lett. 6, 89 (1961)

[46] M. Suenaga, A. F. Clark (eds.), *Filamentary A15 Superconductors*, Plenum Press: New York (1980)

[47] D. Abukay, L. Rinderer, Cryogenics 25, 452 (1985)

[48] G. R. Stewart, Physica C 514, 28 (2015)

[49] Q. Y. Wang et al., Chin. Phys. Lett. 29. 037402 (2012)

[50] J.-F. Ge et al., Nature Mater 13, 285 (2015)

[51] S. Haindl, M. Kidszun, F. Onken, A. Mietke, T. Thersleff, Int. J. Mod. Phys. B 27, 1330001 (2013)

[52] I. Corrales-Mendoza, P. Bartolo-Pèrez, V. M. Sánchez-Reséndiz, S. Gallardo-Hernández, A. Conde-Gallardo, EPL 109, 17007 (2015)

[53] M. Kidszun et al., Phys. Rev. Lett. 106, 137001 (2011)

[54] Yu. G. Naidyuk et al., Supercond. Sci. Technol. 24, 065010 (2011)

[55] X. Xi et al., Phys. Rev. B. 87, 180509 (2013)

[56] S. Haindl, K. Hanzawa, H. Sato, H. Hiramatsu, H. Hosono, *submitted*

[57] S. Haindl, S. Molatta, H. Hiramatsu, H. Hosono, J. Phys. D: Appl. Phys. 49, 345301 (2016)

[58] H. Sugawara, T. Tsuneki, D. Watanabe, A. Yamamoto, M. Sakoda, M. Naito, Supercond. Sci. Technol. 28, 015005 (2015)

[59] D. B. Chrisey, G. K. Hubler (eds.), Pulsed Laser Deposition of Thin Films. Wiley, New York (1994)

[60] H. Hiramatsu, H. Sato, T. Katase, T. Kamiya, H. Hosono, Appl. Phys. Lett. 104, 172602 (2014)

[61] T. Katase, H. Hiramatsu, T. Kamiya, H. Hosono, Supercond. Sci. Technol. 25, 084015 (2012)

[62] J. Engelmann et al., Eur. Phys. J. B. 85, 406 (2012)

[63] S. Molatta, S. Haindl, S. Trommler, M. Schulze, S. Wurmehl, R. Hühne, Sci. Rep. 5, 16334 (2015)

[64] S. X. Huang, C. L. Chien, V. Thampy, C. Broholm, Phys. Rev. Lett. 104, 217002 (2010)

[65] T. Thersleff et al., Appl. Phys. Lett. 97, 022506 (2010)

[66] J. Engelmann et al., Physica C 494, 185 (2013)

[67] K. Iida et al., Appl. Phys. Lett. 97, 172507 (2010)

[68] H. Hiramatsu, T. Katase, T. Kamiya, H. Hosono, IEEE Trans. Appl. Supercond. 23, 7300405 (2013)

[69] S. Adachi, T. Shimode, M. Miura, N. Chikumoto, A. Takemori, K. Nakao, Y. Oshikubo, K. Tanabe, Supercond. Sci. Technol. 25, 105015 (2012)

[70] T. Katase, S. Iimura, H. Hiramatsu, T. Kamiya, H. Hosono, Phys. Rev. B 85, 140516 (2012)

[71] T. Katase, H. Hiramatsu, T. Kamiya, H. Hosono, New. J. Physics 15, 073019 (2013)

[72] J. Yong, S. Lee, J. Jiang, C. W. Bark, J. D. Weiss, E. E. Hellstrom, D. C. Larbalestier, C. B. Eom, T. R. Lemberger, Phys. Rev. B 83, 104510 (2011)

[73] B. Gorshunov, D. Wu, A. A. Voronokov, P. Kallina, K. Iida, S. Haindl, F. Kurth, L. Schultz, B. Holzapfel, M. Dressel, Phys. Rev. B 81, 060509 (2010)

[74] A. E. Karakozov, S. Zapf, B. Gorshunov, Ya. G. Ponomarev, M. V. Magnitskaya, E. Zhukova, A. S. Prokhorov, V. B. Anzin, S. Haindl, Phys. Rev. B 90, 014506 (2014)

[75] T. Fischer, A. V. Pronin, J. Wosnitza, K. Iida, F. Kurth, S. Haindl, L. Schultz, B. Holzapfel, E. Schachinger, Phys. Rev. B 82, 224507 (2010)

[76] D. Kasinathan, A. Ormeci, K. Koch, U. Burkhardt, W. Schnelle, A. Leithe-Jasper, H. Rosner, New J. Physics 11, 025023 (2009)

[77] We will write here $H_{c2,ab}$ although the unit cell is tetragonal and $a = b$ holds.

[78] S. A. Baily, Y. Kohama, H. Hiramatsu, B. Maiorov, F. F. Balakirev, M. Hirano, H. Hosono, Phys. Rev. Lett. 102, 117004 (2009)

[79] F. Hunte et al., Nature 453, 903 (2008)

[80] J. Jaroszynski etl al., Phys. Rev. B 78, 174523 (2008)

[81] H.-S. Lee et al., Phys. Rev. B 80, 144512 (2009)

[82] N. D. Zhigadlo et al., J. Phys. Condens. Matter 20, 342202 (2008)

[83] E. Helfand, N. R. Werthamer, Phys. Rev. Lett. 13, 686 (1964); E. Helfand, N. R. Werthamer, Phys. Rev. 147, 288 (1966); N. R. Werthamer, E. Helfand, P. C. Hohenberg, Phys. Rev. Lett. 147, 295 (1966)

[84] A. Gurevich et al., Supercond. Sci. Technol. 17, 278 (2004)

[85] A. Gurevich, Phys. Rev. B 67, 184515 (2003)

[86] G. Blatter, V. B. Geshkenbein, A. I. Larkin, Phys. Rev. Lett. 68, 875 (1992)

[87] L. Civale et al., J. Low Temp. Phys. 135, 87 (2004)

[88] V. G. Kogan, R. Prozorov, Rep. Prog. Phys. 75, 114502 (2012)

[89] F. Kurth et al., Supercond. Sci. Technol. 26, 025014 (2013)

[90] N. Ni et al., Phys. Rev. B 78, 214515 (2008)

[91] J.-H. Chu et al., Phys. Rev. B 79, 014506 (2009)

[92] F. L. Ning et al., Phys. Rev. Lett. 104, 037001 (2010)

[93] R. M. Fernandes et al., Phys. Rev. B 85, 140512 (2012)

[94] N. Ni et al., Phys. Rev. B 78, 214515 (2008)

[95] M. Kano et al., J. Phys. Soc. Jpn 78, 084719 (2009).

[96] V. A. Gasparov et al., Pisma ZhETF 93, 746 (2011).

[97] M. A. Tanatar et al., Phys. Rev. B 79, 094507 (2009)

[98] Z. Wang et al., Phys. Rev. B 92, 174509 (2015)